Protist 181 (2026) 126159

Contents lists available at ScienceDirect

Protist

journal homepage: www.elsevier.de/protis

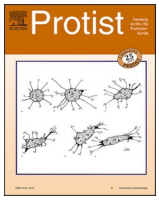

Genetic engineering of dinoflagellate algae and the lethality of an introduced plastid terminal oxidase☆

I.C. Nimmo [a,b], C.E. Evans [c], L.M. Li [d], A.C. Barbrook [a], K. Geisler [e], F.H. Kleiner [c,f], A. Scarampi [a,g], D. Kosmützky [a,h], L.T. Wey [a,i], R.G. Dorrell [d], C.J. Howe [a,1], R.E.R. Nisbet [c,*,1]

[a] Department of Biochemistry, University of Cambridge, Tennis Court Rd, Cambridge CB2 1QW, UK
[b] current: Cambridge Institute of Therapeutic Immunology and Infectious Disease, Jeffrey Cheah Biomedical Centre, University of Cambridge, Puddicombe Way, Cambridge CB2 0AW, UK
[c] School of Biosciences, University of Nottingham, Sutton Bonington Campus, Loughborough, Leicestershire LE12 5RD, UK
[d] Computational, Quantitative and Synthetic Biology (CQSB), UMR7238, Centre Nationale de la Recherche Scientifique (CNRS), Institut de Biologie Paris-Seine (IBPS), Sorbonne Université, 75005 Paris, France
[e] Department of Plant Sciences, University of Cambridge, Downing Street, Cambridge CB2 3EA, UK
[f] current: Department of Bionanoscience, Delft University of Technology, Gebouwnummer 58, Van der Maasweg 9, 2629, HZ, Delft, the Netherlands
[g] current: School of Life Sciences, University of Warwick, Coventry CV4 7AL, UK
[h] current: Sainsbury Laboratory, University of Cambridge, CB2 1LR, UK
[i] current: Molecular Plant Biology Unit, University of Turku, Tykistökatu, Turku 20520, Finland

ARTICLE INFO

Editor: Genoveva F. Esteban

ABSTRACT

Dinoflagellate algae are a diverse group of single-celled eukaryotes, often living in marine environments. The majority of species are entirely free-living, but many can become symbionts with corals, jellyfish and other marine organisms. With rising sea temperatures, the function of the dinoflagellate photosynthetic machinery, and the redox state of the photosynthetic electron transport chain are impaired. This photosynthetic impairment is likely to be an important cause of coral bleaching. In the chloroplasts of plants and many algae, disturbance of the chloroplast redox state can be in part alleviated by the Plastid Terminal Oxidase protein (PTOX). Here, we made use of our newly developed genetic modification tools in the free-living dinoflagellate species *Amphidinium carterae*, which is found in both in temperate and tropical waters. We test if the introduction of PTOX to the chloroplast would allow *A. carterae* to withstand temperature stress. We find that the expression of the PTOX gene caused a lethal phenotype. Genetic engineering of dinoflagellate algae has long been problematic, and the ability to express heterologous proteins represents a significant advance in the long-term quest to engineer a heat-tolerant dinoflagellate.

1. Introduction

Dinoflagellates are an ancient and diverse group of eukaryotic algae, and are important phytoplankton in the world's oceans. Most species are free-living, while others form ecologically significant symbioses. Many dinoflagellates live at the upper extremity of their temperature zone, and so are extremely susceptible to slight rises in sea water temperature (Gierz et al., 2017; Warner et al., 1999). Dinoflagellates from the Symbiodinaceae family are essential algae in coral reefs, forming a symbiosis with the coral (animals from the phylum Cnidaria) (LaJeunesse et al., 2018). These algae provide 90% of the nutritional needs of the coral through photosynthesis (Muscatine and Porter, 1977). If sea temperatures rise to 30–32 °C, the symbiosis between Cnidaria and the dinoflagellate breaks down. The breakdown of this symbiotic relationship causes coral bleaching and if complete can ultimately cause death of the reef. The loss of coral reefs due to coral bleaching is one of the most pressing environmental challenges facing the world today (Weis, 2008).

There is presently much interest in attempting to confer resistance to stress in dinoflagellate algae. Photoinhibition of coral-associated dinoflagellate algae (family Symbiodiniaceae) has been identified as one

☆ This article is part of a Special issue entitled: 'Dinoflagellates' published in Protist.

* Corresponding author.
E-mail address: Ellen.Nisbet@nottingham.ac.uk (R.E.R. Nisbet).

[1] joint last author

https://doi.org/10.1016/j.protis.2026.126159
Received 4 July 2025; Received in revised form 18 February 2026; Accepted 23 February 2026
Available online 2 April 2026

trigger of coral bleaching (Helgoe et al., 2024). Whilst the exact mechanism of heat-induced photoinhibition in symbiotic dinoflagellates has not been confirmed, it is clear that overreduction of the plastid electron transport chain (PETC) and reactive oxygen species (ROS) are involved (reviewed by (Szabó et al., 2020)). A proposed mechanism includes ROS production as a result of heat inactivation of the Type II ribulose-1,5-bisphosphate carboxylase-oxygenase (RuBisCO) that dinoflagellates contain. This enzyme is heat intolerant; and stops working above about 30 °C (Lilley et al., 2010). When RuBisCO activity ceases, the Calvin–Benson–Bassham (CBB) cycle is also inhibited. This causes overreduction of the photosynthetic electron transport chain, including the plastoquinone pool, the generation of ROS and photoinhibition at Photosystem II (PSII) (Foyer and Hanke, 2022; Ragni et al., 2010; Jones et al., 2000; Warner et al., 1999). Understanding how dinoflagellates respond to heat stress is a fundamental question, and one that urgently needs answering.

The plastid terminal oxidase (PTOX) is a protein found in the chloroplast of plants and many eukaryotic algae (Fig. 1). The protein is also found in some cyanobacterial species, where it is called the plastid-like terminal oxidase. PTOX is a plastoquinol oxidase, located on the stromal side of the thylakoid (Lennon et al., 2003). It is believed to have dual roles in carotenoid biosynthesis and in adjusting the redox poise of the photosynthetic electron transport chain (PETC) by oxidising the plastoquinone (PQ) pool (Joët et al., 2002). Although it has been suggested this may help avoid the generation of ROS, under some conditions PTOX may result in ROS generation (Heyno et al., 2009; Joët et al., 2002). Previous work has shown that levels of PTOX may increase in photosynthetic organisms under stress conditions (Stepien and Johnson, 2009; Shahbazi et al., 2007; Streb et al., 2005). It is therefore proposed that the protein may provide a safety valve for survival under high light, high temperature or high salt conditions (Shahbazi et al., 2007). Our searches of the sequenced dinoflagellate genomes and transcriptomes available via the NCBI revealed that these algae may contain a gene for PTOX, although none has been confirmed experimentally.

Several groups have genetically modified plants to express elevated levels of PTOX, in an attempt to confer resistance to stress conditions (Ahmad et al., 2012; Rosso et al., 2006). However, the consequences of overexpression have differed among studies, and in some instances overexpression has led to increased photoinhibition (Heyno et al., 2009).

To date, efforts to understand dinoflagellate biology have been primarily correlative, due to the absence of a robust genetic transformation system, and the complexity of the genome. Due to the evolutionary distances from model species, many genes remain unannotated. This makes it hard to determine the function and role of proteins (Lin, 2024). However, recent molecular advances have transformed the field, including nuclear transformation in *Breviolum minutum* (Gornik et al., 2022) and long-term expression of heterologous genes in *Oxyrrhis marina* (Sprecher et al., 2020). In 2019, we established the first stable genetic modification system in dinoflagellate chloroplasts, using *Amphidinium carterae* (Nimmo et al., 2019). *A. carterae* has been used as a model organism for dinoflagellates as it lacks the armoured thecal plates common in other species. These thecal plates have been proposed to be one reason why genetic transformation of dinoflagellates has proved difficult (Chen et al., 2019). Most cultured *Amphidinium* strains are temperate and coastal isolates (e.g.; CCMP1314, from Falmouth Pond, Massachusetts, USA) and are maintained at 19–21 °C, although prior physiological studies have indicated that some subpopulations may survive at up to 30 °C (Aquino Cruz and Okolodkov, 2016).

To establish transformation in *A. carterae*, we made use of the unique fragmented dinoflagellate chloroplast genome. Instead of having a conventional 120–150 kb circular chloroplast genome, many dinoflagellate species have a fragmented chloroplast genome of approximately 20 plasmid-like minicircles (Howe et al., 2008). Dependent on species, each minicircle contains between 0 and 4 genes and is up to 5 kb in size. Each contains a conserved core region containing the origin of replication and transcriptional start site (Howe et al., 2008). By replacing the protein-coding gene in the *psbA* or *atpB* minicircles with a selectable marker, we were able to create artificial minicircles for genetic transformation (Faktorová et al., 2019; Nimmo et al., 2019). With the advent of a stable transformation system, allowing expression of heterologous genes, we can at last study these enigmatic algae at a molecular level. Although *A. carterae* is likely not a symbiotic species, the knowledge gained from a tractable, model system could give rise to significant insights in other, as-yet intractable systems, such as the Symbiodiniaceae.

This study aimed to make use of these newly developed genetic modification tools to overexpress PTOX in the *A. carterae* chloroplast. We proposed that overexpression of PTOX would help the algae withstand heat stress more effectively. The presence of PTOX may relieve the heat-induced overreduction of the PQ pool and subsequent PSII photoinhibition.

Here, we first assess the spatial distribution of wild relatives of *A. carterae*, suggesting it can occur in environmental temperatures up to 30 °C. Next, we present further artificial minicircles, suitable for introducing genes into the dinoflagellate chloroplast. One is based on the *petD* minicircle, and the other is based on the minicircle containing *petB* and *atpA* genes, designed to express two transgenes in parallel. We make use of this two-gene construct to introduce the *Arabidopsis thaliana* PTOX coding sequence into *A. carterae*. We find that the PTOX gene confers a lethal phenotype, killing the cells within 14 days. We conclude that the heterologous expression of PTOX in the chloroplast (at least under the strong promoters used here) is not able to confer heat tolerance in dinoflagellates.

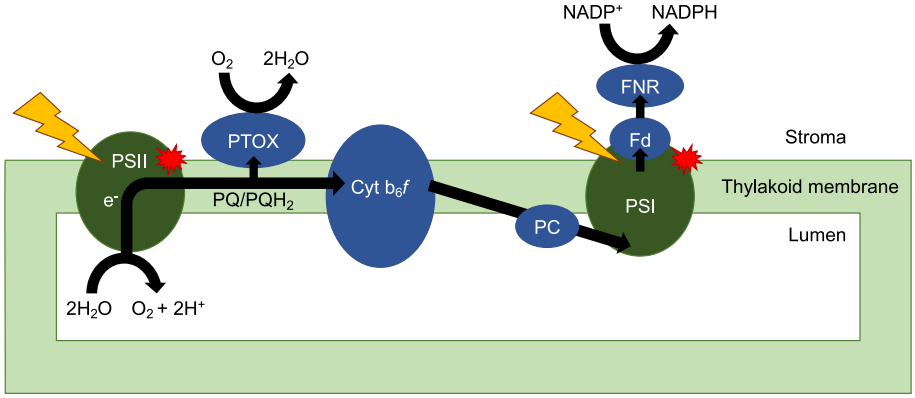

Fig. 1. A schematic electron transfer pathway in dinoflagellate chloroplasts. Abbreviations: PSI: Photosystem I; PSII: photosystem II; e^-: electron; PTOX: plastid terminal oxidase; PQ/PQH_2: plastoquinone pool; cyt b_6f: cytochrome b_6f complex; PC; plastocyanin; Fd: ferredoxin; FNR: ferredoxin NADP reductase. Yellow arrow: light, red star: sites of photoinhibition.

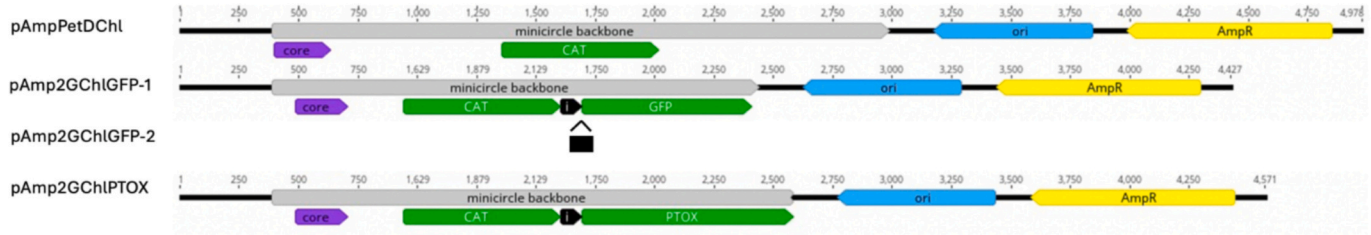

Fig. 2. Linearized artificial minicircles pAmpPetDChl, pAmp2GChlGFP-1, pAmp2GChlGFP-2 and pAmp2GChlPTOX. The grey arrow indicates the region originating from a minicircle, the remainder is bacterial shuttle vector (based on the *E. coli* vector pMA). The bacterial origin of replication (*ori*) is blue and the minicircle core region (core) is purple. AmpR (yellow) is the region encoding ampicillin resistance for selection in *E. coli* and CAT (green) encodes chloramphenicol acetyl transferase, for selection in *A. carterae*. GFP (green) and PTOX (green) are both codon optimized for *A. carterae*. The intergenic region (black) is the region between *petB* and *atpA*. pAmp2GChlGFP-1 has the intergenic region as originally annotated, while pAmp2GChlGFP-2 contains an additional 120 bp at the 3′ end of the intergenic region. The additional 120 bp is shown as a black box, and its insertion point is indicated. (For interpretation of the references to colour in this figure legend, the reader is referred to the web version of this article.)

2. Methods

2.1. Distribution of A. carterae

Spatial distributions of *A. carterae*, and the close relatives *A. operculatum* and *A. simplex* were assessed using 18S V4 rDNA Amplicon Sequence Variants (ASVs) located in the *Tara* Oceans Barcode Atlas and in MetaPR2 via a previously defined phylogenetic reconciliation pipeline (Vernette et al., 2021; Vaulot et al., 2022; Perrin and Dorrell, 2024). Briefly, a reference library of dinoflagellate 18S rDNA sequences was assembled from GenBank (accessed April 2025) and from nucleotide transcriptomes from the MMETSP database (Dorrell et al., 2017), and this was then enriched with all *Tara* Ocean Barcode Atlas and MetaPR2 database ribotypes annotated as belonging to *Amphidinium*. The library was aligned using MAFFT v7.90 under the –auto and –adjustdirection settings, and the alignment was trimmed with TrimAl using setting -gt 0.5 (Katoh and Standley, 2013; Capella-Gutiérrez et al., 2009). The trimmed alignment was parsed with IQ-TREE (Nguyen et al., 2015) using -st DNA -nt AUTO -lmap 2000 -con -bb 1000 settings, and the consensus tree was parsed for MetaPR2 ribotypes showing greater proximity to annotated *A. carterae, A. operculatum* or *A. simplex* than to other dinoflagellates. Alignments, phylogenies, and spatial distributions of all identified *A. carterae* meta-genes are provided in Dataset S1. Flatfiles (tab-separated text files, pdf figures) of each sheet in Dataset S1 are provided at the following open-access Zenodo repository: https://doi.org/10.5281/zenodo.18555380

2.2. Culturing of A. carterae

A. carterae CCMP1314 was grown in f/2 medium on a 16/8 h light/dark cycle at 18 °C at 30μE m^{-2} s^{-1}, as previously described (Barbrook et al., 2006). Cells under high or low light were grown at 18 °C at 60 μE m^{-2} s^{-1} or 15 μE m^{-2} s^{-1} respectively, under the same 16 h:8 h light: dark cycle.

2.3. Vector construction and transformation

All constructs were based on native *A. carterae* chloroplast DNA minicircles, following Nimmo et al., 2019. The pAmpChl and pAtpBChl constructs are described in Nimmo et al., 2019 and Faktorová et al., 2019. For the novel construct pAmpPetDChl, the *petD* gene in the *petD*-containing minicircle (AJ250265) was replaced with a sequence encoding chloramphenicol acetyl transferase (*CAT,* codon optimized for *A. carterae* (Barbrook and Howe, 2000)), and linearized after the end of *CAT* for cloning into the *E. coli* shuttle vector pMA. The pAmp2GChlGFP-1 construct is based on the *petB/atpA* minicircle (AY048664). The *petB* gene was replaced with *CAT* and the *atpA* gene was replaced with a sequence encoding green fluorescent protein (*eGFP*, codon optimized for *A. carterae*). As the annotation of the *petB/atpA* minicircle contains an uncertain annotated start codon for *atpA* (Barbrook et al., 2001), a second construct based on this minicircle was also designed, entitled pAmp2GChlGFP-2. This construct assumed *atpA* commenced at position 1457 instead of 1337 (numbering as in AY048664). It therefore has an an extra 120 bp intergenic region between *petB* and *atpA*. As before, the *petB* gene was replaced with *CAT,* and the *atpA* gene was replaced with a sequence encoding green fluorescent protein (*eGFP*; codon optimized for *A. carterae*). Finally, we created the construct pAmp2GChlPTOX, replacing *GFP* in pAmp2GChlGFP-1 with *PTOX* from *Arabidopsis thaliana* (Genbank: NP567658). As PTOX is encoded in the nuclear genome, it contains a chloroplast-targeting sequence. The sequence encoding this was removed, and the remaining gene codon optimized for *A. carterae* (Barbrook and Howe, 2000). Sequences were synthesized by GeneArt (Invitrogen) and inserted into the *E. coli* pMA cloning vector, or, for pAmp2GChlGFP-2 only, synthesized by Twist Bioscience and inserted into pTwist Amp High Copy. The constructs are shown in Fig. 2, and sequences for all construct sequences are given in Suppl. data.2.

Transformation was carried out either following Nimmo et al. (2019), using a Bio-Rad Biolistics PDS-1000/He system or using electroporation. In the former case, approx. 2.5×10^7 early log phase cells were used in each transformation experiment, with 1550 psi rupture disks. Antibiotic selection (in liquid media) was imposed on day 3 with the addition of chloramphenicol at a final concentration of 20 μg ml^{-1}. Each transformation experiment was carried out in triplicate. Transformed cells were grown under normal light intensity (30 μE m^{-2} s^{-1}). Where noted transformed cells were also grown at 15 μE m^{-2} s^{-1} or 60 μE m^{-2} s^{-1}. A full protocol can be found at https://www.protocols.io/view/biolistic-transformation-of-amphidinium-4r2gv8e. Electroporation experiments were carried out using the Lonza system, as previously described (Gornik et al., 2022), with antibiotic selection as above.

2.4. RT-PCR

The total *A. carterae* cell population at day 7 post-transformation (approx. 5×10^6 cells) was harvested in a benchtop centrifuge for analysis by RT-PCR. Total RNA was isolated using the Trizol - chloroform method as previously described (Nimmo et al., 2019). 1 ml Trizol was added to each cell pellet, and RNA was isolated following the manufacturer's instructions (Invitrogen). Extracted RNA was subjected to an on-column DNase treatment, following the Qiagen RNeasy kit protocol. First strand synthesis was performed using Invitrogen SuperScript IV using the manufacturer's protocol, with gene-specific reverse primers. The cDNA was used in PCR with GoTaq (Promega) or DreamTaq (ThermoFisher) polymerase according to the manufacturer's instructions.

2.5. Primer sequences

CAT-1: Fwd: CGCCTTTCGAACGACG, Rev.: AGGACTAATGATAGTCTCCCG, with a T_m of 52 °C giving rise to a 324 bp product. pAmpPetDChl: Fwd: CGACAGGAGTGATTAACTGAG, Rev.: GGAATG CGGTGATATCAAGCTGTACTG, giving rise to a 1061 bp product. pAmp2GChlGFP: Fwd: GGAATGCGGTGATATCAAGCTGTACTG, Rev.: CGGAACTCTGGATGTGCG giving rise to a 430 bp product. CAT_F2: GCTTGATATCACCGCATTCC, CAT_R3: TAACGTCGCGAACATGGACA, giving rise to a 380 bp product. GFP_F1: TCTGCAATGCCAGAGGGTTA, GFP_R1: GATGGTGGTGTACAGCTTGC, giving rise to a 281 bp product. Primers for PTOX: Fwd: GAAGGCATCAGGCGAG, Rev.: CAGTGTG CCTCCTCTGG, with a T_m of 52 °C, giving rise to a 300 bp product.

2.6. Western blot

A. carterae cell lysates were extracted from mature cultures of wild type and transformant lines grown in f/2 without selection, by incubation in extraction buffer [50 mM Tris-HCl (pH 6.8), 2% (*w/v*) SDS, and incubated with cOmplete protease inhibitor cocktail (Sigma-Aldrich)] for 30 min at room temperature, followed by centrifugation, where supernatant was collected. The lysate was denatured in sample buffer for 10 min at 95 °C before SDS-PAGE. Western blots, following blocking in TBS-T 5% milk powder, were probed with monoclonal anti-GFP antibody raised in mouse (Sigma G6539), and HRP-conjugated secondary antibody (Invitrogen 31,430).

3. Results

3.1. Distribution and wild thermal niche of A. carterae

To assess the probable thermal tolerance of *A. carterae* in the wild, we considered its likely habitats, together with those of the conspecific *A. operculatum* and the sister-group *A. simplex*, using meta-barcoding data normalized in the *Tara* Ocean Barcode Atlas and MetaPR2 servers and a previously defined phylogenetic reconciliation pipeline (Fig. 3) (Vaulot et al., 2022; Perrin and Dorrell, 2024). Eight MetaPR2 Allele Specific Variants (ASVs, corresponding to taxonomically distinct 18S rDNA sequences) and 45 *Tara* Oceans ASVs related to *A. carterae* were identified, with individual distributions shown in Dataset S1. Different spatial distributions were observed for *A. carterae* in MetaPR2, in which it was found in both temperate and tropical coastal stations (Pacific Northwest, Bay of Bengal, Fig. 4), and in *Tara* Oceans ASVs, where it was

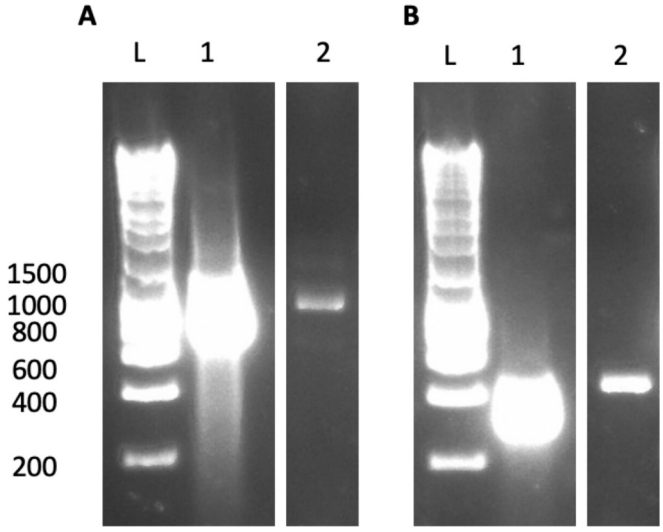

Fig. 4. PCR to test for successful transformation. A. pAmpPetDChl (pAmpPetDChl primer pair), **B**. pAmp2GChlGFP-1 (pAmp2GChlGFP primers). Lane L, hyperladder 1kB (Bioline), Lane 1 positive control (purified transformation vector), Lane 2, DNA isolated from putative transformed *A. carterae*.

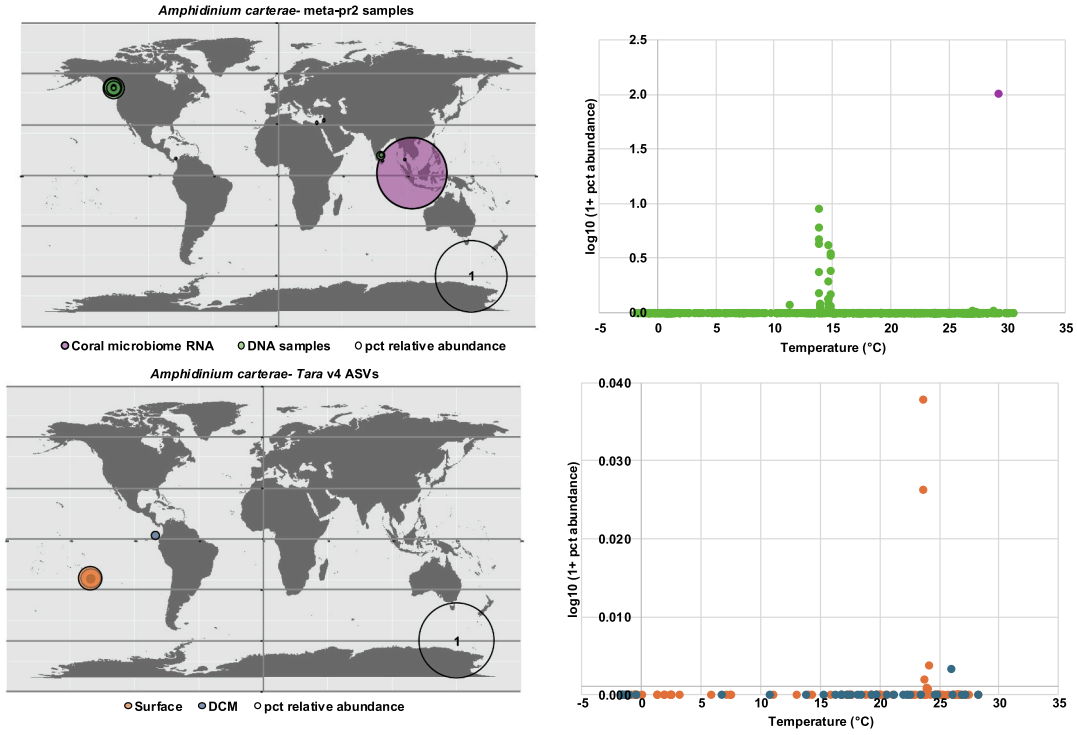

Fig. 3. Spatial distribution and thermal niche of environmental *Amphidinium carterae*meta-genes. Left: a map of total relative abundance (expressed as pct: per 250 mappedribotypes) of (1) MetaPR2 samples and (2) *Tara* Oceans v4 ASVs, across all depths and 0.8–2000 µm size fractions, that could be phylogenetically reconciled to *Amphidinium carterae/ A. operculatum/ A. steinii*, following methodology of Perrin and Dorrell (2024). Right: measured temperature of each site, showing thermal niches from 13 to 15 °C (MetaPR2) or 23–27 °C (*Tara*). Plots of individual size fractions are provided in Fig. S1 and phylogenies in Fig. S2.

widespread but at low abundance across the subtropical ocean. A detailed view of individual *Tara* Oceans size fractions particularly suggested occurrence of *A. carterae*-related ASVs in surface and nano-sized fractions (5–180 μm) in the subtropical Pacific and Indian Ocean (Fig. S1). With regard to thermal niche, the Pacific Northwest stations in which MetaPR2 ASVs were identified had moderate measured temperatures (11.31–14.81 °C), consistent with the collection site of the type culture CCMP1314 (Nantucket Sound, USA; Wangersky and Guillard, 1960). In contrast; the subtropical and Indian Ocean stations in which *A. carterae*-related sequences were detected were warmer (c. 25–28 °C, Dinesh Kumar et al., 2016), suggesting a capacity for thermotolerance in this species or its close relatives which may render it an appropriate model for laboratory study.

Three of the *A. carterae* MetaPR2 ASVs, forming a monophyletic subclade (7801b4db34, 157087fad5, 14928aaaac) were detected as abundant in one coral reef microbiome, with measured sea temperature 29.3 °C (Fig. 3, S2). This is unlikely to be due to biological or technical contamination as the most closely-related ASVs to this clade in Tara Oceans are likewise detected in coral-associated environments from the Western Indian Ocean (Juan de Nova Island) and Eastern Pacific Oceans (Mangareva Islands). It is nonetheless unlikely that *A. carterae* is a true coral endobiont, with previous studies collecting *Amphidinium* as a benthic and epibiotic dweller in reef environments (Durán-Riveroll et al., 2023). Further confirmation of the *Amphidinium* environmental niche will be best explored by mapping its sequenced genome onto shotgun total meta-genomic sequencing data from wild habitats (Judd et al., 2024).

3.2. Development of new transformation vectors

We designed two new artificial minicircles as transformation vectors, pAmpPetDChl and pAmp2GChlGFP-1. The pAmpPetDChl vector is based on the *petD* single gene minicircle, while the pAmp2GChlGFP vector is based on the two-gene minicircle containing *petB* and *atpA*. Each artificial minicircle has an *E. coli* pMA plasmid backbone, and contains the full *A. carterae* minicircle sequence, with either the *petD* or *petB* coding sequences replaced with a sequence encoding chloramphenicol acetyl transferase (CAT, and indicated by 'Chl' in the vector name). In the two-gene minicircle, the *atpA* gene is replaced with one for eGFP. These vectors are designed to allow selection in *E. coli* with ampicillin, and for selection in *A. carterae* with chloramphenicol. Note that selection in *E. coli* with chloramphenicol was not successful.

To determine if there was a difference in transformation success rates (defined as the fraction of transformation experiments that gave rise to antibiotic-resistant cells) between artificial minicircles, *A. carterae* cells were bombarded with each artificial minicircle multiple times, followed by selection with chloramphenicol, as shown in Table 1. PCR to test for the presence of each artificial minicircle was carried out following each transformation (Fig. 4). We included our two previously published minicircles pAmpChl (based on the *A. carterae psbA* minicircle (Nimmo et al., 2019)) and pAmpAtpBChl (based on the *A. carterae atpB* minicircle (Faktorová et al., 2019)) for comparison. Although the success rates (number of discrete transformation attempts recovering at least some chloramphenicol-resistant cell lines) varied from 33% to 75%, there was no statistically significant difference between vectors (Chi-squared, $p = 0.05$), as shown in Table 1. All transformation experiments using the Lonza electroporator were unsuccessful ($n = 9$, using the pAmpChl artificial minicircle).

Table 1
Efficiency of biolistic transformation. Each artificial minicircle was used to transform wild type *A. carterae* in separate biolistic transformations. The number of times that cultures contained transformed cells (as confirmed by PCR) was recorded. Each transformation experiment (or set of experiments) also included a no vector control, to ensure that cells survived the biolistic procedure. Transformations were carried out at both the University of Cambridge and University of Nottingham by separate individuals, and transformants were obtained at both sites.

Artificial minicircles	Original minicircle	Size (bp)	Times shot	Successful transformation	% success
pAmpChl	*psbA*	4326	12	9	75%
pAmpAtpBChl	*atpB*	3870	9	4	44%
pAmpPetDChl	*petD*	4978	9	3	33%
pAmp2GChlGFP-1	*atpA/petB*	4427	13	5	39%

3.3. Effect of artificial minicircles on A. carterae growth rate

To determine if the introduction of artificial minicircles affected the growth rate of *A. carterae,* cultures of each of the four lines (pAmpChl, pAmpAtpBChl, pAmpPetDChl and pAmp2GChlGFP-1) were established in triplicate (from separate transformation events), and grown in standard conditions in the presence of chloramphenicol for 21 days. This showed that the strains containing pAmpChl and pAmpAtpB had similar growth rates, while strains containing the pAmpPetDChl and pAmp2GChlGFP-1 grew at substantially lower rates, Fig. 5.

We tested if average growth rates of cells over 21 days with the chloramphenicol resistance gene replacing different endogenous genes correlated with the transcript levels of the endogenous genes in wild type cells. The growth rate of cultures resulting from transformation with each artificial minicircle was compared with known transcript levels of each native minicircle, as shown in Table 2. The transcript level data were obtained from the same strain in our laboratory (Cambridge) in previous experiments (Dorrell et al., 2019). The results showed that cultures transformed with plasmids based on minicircles corresponding to more abundant transcripts (pAmpPetDChl, pAmp2GChlGFP-1) grew more slowly than cultures containing plasmids based on minicircles with less abundant transcripts (pAmpChl and pAmpAtpBChl).

3.4. Expression of GFP in A. carterae containing pAmp2GChlGFP

To determine if the GFP gene was expressed from the two-gene minicircle, pAmp2GChlGFP-1, we used RT-PCR with RNA extracted from three independent cultures transformed with the plasmid and selected with chloramphenicol, as shown in Fig. 6. This confirmed RNA transcripts encoding GFP were present.

RNA was extracted from wild type *A. carterae* (lanes 1–3) and cells containing pAmp2GChlGFP-1 (lanes 4–6). A RT-PCR reaction was carried out using primers against GFP (primer pair GFP-1), with or without reverse transcriptase (+RT, −RT) as shown. Lanes + and – show the results of PCR with the same primers with (+) or without (−) purified vector as DNA template.

Despite the presence of mRNA encoding GFP, it was not possible to detect functional GFP via fluorescence wide-field microscopy, and the absence of GFP was confirmed in a western blot (Fig. 7). Although we initially speculated that this could be due to high levels of autofluorescence (Tang and Dobbs, 2007), we realised that the original annotation of the *petB-atpA* minicircle was inconclusive concerning the position of the *atpA* start codon (Barbrook et al., 2001). As the *GFP* gene in the pAmp2GChlGFP-1 construct was placed in the same position on the minicircle as *atpA,* an incorrect annotation for *atpA* would result in an incorrect positioning of *GFP*. We therefore re-analyzed the *petB-atpA* minicircle sequence. Alignments with other *atpA* genes revealed that the *A. carterae* gene (as annotated) had an extended N-terminal coding region not present in other species. Additionally, ribosomal binding site (RBS) prediction software designed for cyanobacteria (as a proxy for chloroplasts) did not predict a RBS upstream of the presumed initiation codon for *atpA* (Reis and Salis, 2020). Instead, there was a strong predicted RBS 120 bp downstream, consistent with the start of alignment with other *atpA* genes. Together, these results would indicate that the intergenic region between *petB* and *atpA* is 120 bp longer than originally annotated (Barbrook et al., 2001).

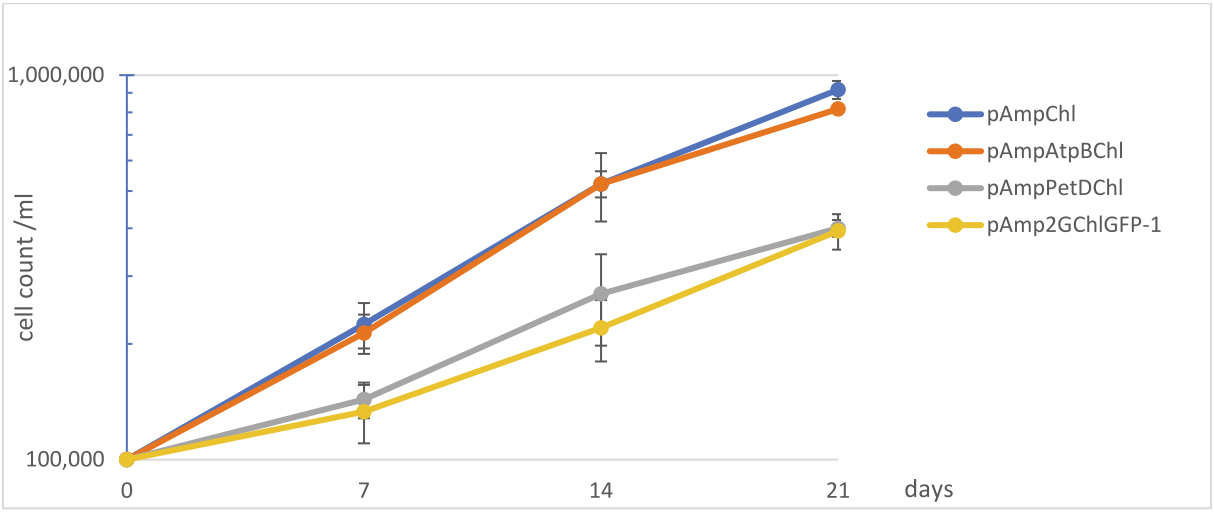

Fig. 5. Growth curves. The four transformed cell lines were grown (in triplicate) in the presence of chloramphenicol for 21 days. Cell counts were undertaken using a haemocytometer at days 7, 14 and 21. The original minicircle on which each construct was based is shown. All cultures contained 100,000 cells at day 0. Note that untransformed cells do not grow under chloramphenicol selection.

Table 2
Expression of CAT in artificial minicircles. As a comparison, the levels of expression of the native minicircle from wild type cells are taken from (Dorrell et al., 2019).

artificial minicircle	native minicircle	expression level of native gene (mean read coverage)	doubling time (days)
pAmpChl	*psbA*	810	6.6
pAmpAtpBChl	*atpB*	670	6.9
pAmpPetDChl	*petD*	1470	10.5
pAmp2GChlGFP-1	*atpA/petB*	1250	10.7

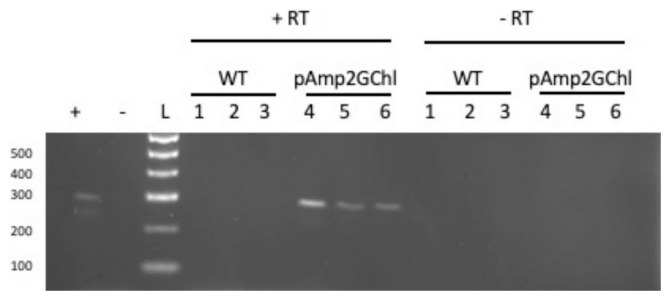

Fig. 6. Expression of GFP mRNA in cells containing *pAmp2GChlGFP-1*.

We therefore redesigned the artificial minicircle containing GFP to contain the new, 120 bp longer intergenic region, as pAmp2GChlGFP-2. This artificial minicircle was introduced into *A. carterae* using biolistics, and following selection, we were able to identify the minicircle using PCR 60 days after transformation, indicating stable transformation (Fig. 7A). However, RT-PCR to show transcription of GFP was not successful (Fig. 7B), nor were western blots (Fig. 7C), suggesting that the GFP protein was not expressed in the cell.

3.5. Presence of a PTOX gene is lethal in A. carterae

We wished to test if the introduction of PTOX would confer heat resistance to *A. carterae*. We therefore removed the gene encoding GFP from the pAmp2GChlGFP-1 artificial minicircle and replaced it with a codon-optimized *PTOX* from *A. thaliana*, as shown in Fig. 2. Although there is a possible RBS upstream of *PTOX* in the vector, there is also a strong RBS at the 5′ end of the recoded PTOX gene, within the coding sequence (Reis and Salis, 2020). This would allow synthesis of PTOX with a 12 aa N-terminal truncation.

We used biolistic transformation to introduce the pAmp2GChlPTOX construct into *A. carterae*. Despite attempting the transformation with pAmp2GChlPTOX nine times in triplicate (i.e., a total of 27 independent transformation attempts), the *A. carterae* cells never survived more than 14 days post-transformation, as judged by a failure to observe motile cells by light microscopy. Cultures were followed for a further two weeks by which time no intact cells were visible. As a positive control, *A. carterae* cells were transformed in parallel with pAmpChl (which confers resistance to chloramphenicol (Nimmo et al., 2019)), and these cells remained alive at 14 days under selection with chloramphenicol, as judged by light microscopy. As a negative control, *A. carterae* cells were transformed with the *E. coli* cloning vector pGEM-T easy. These cells all died within 14 days under chloramphenicol selection, as expected. Together these results indicate that the introduction of PTOX was lethal to the recipient cells.

3.6. Confirmation of transcription of PTOX in A. carterae

To confirm that PTOX was indeed transcribed prior to the death of *A. carterae* cells, we re-transformed cells with pAmp2GChlPTOX and harvested RNA after 7 days, before the cells had died (as judged by the presence of motile cells by light microscopy). RT-PCR was carried out using a set of primers within the PTOX coding sequence, and a set of primers within the coding sequence of the selectable marker, CAT. RT-PCR products of the expected sizes were seen for PTOX and for CAT (Fig. 8), and these were confirmed by sequencing. No products were seen in negative controls without reverse transcriptase, or in lines transformed with the *E. coli* vector pGEM-T easy, which does not carry either of those coding sequences and is not expected to replicate in the dinoflagellate chloroplast. We were unable to carry out any biophysical measurements of photosynthesis function (e.g. PAM fluorometry of chlorophyll fluorescence) or biochemical measurements of photosynthetic machinery (e.g. western blots of photosystem proteins), as there was insufficient cellular material.

3.7. Effect of PTOX in A. carterae under high and low light conditions

Previous studies have shown that the consequences of PTOX expression depend on the light intensity to which cells are subjected

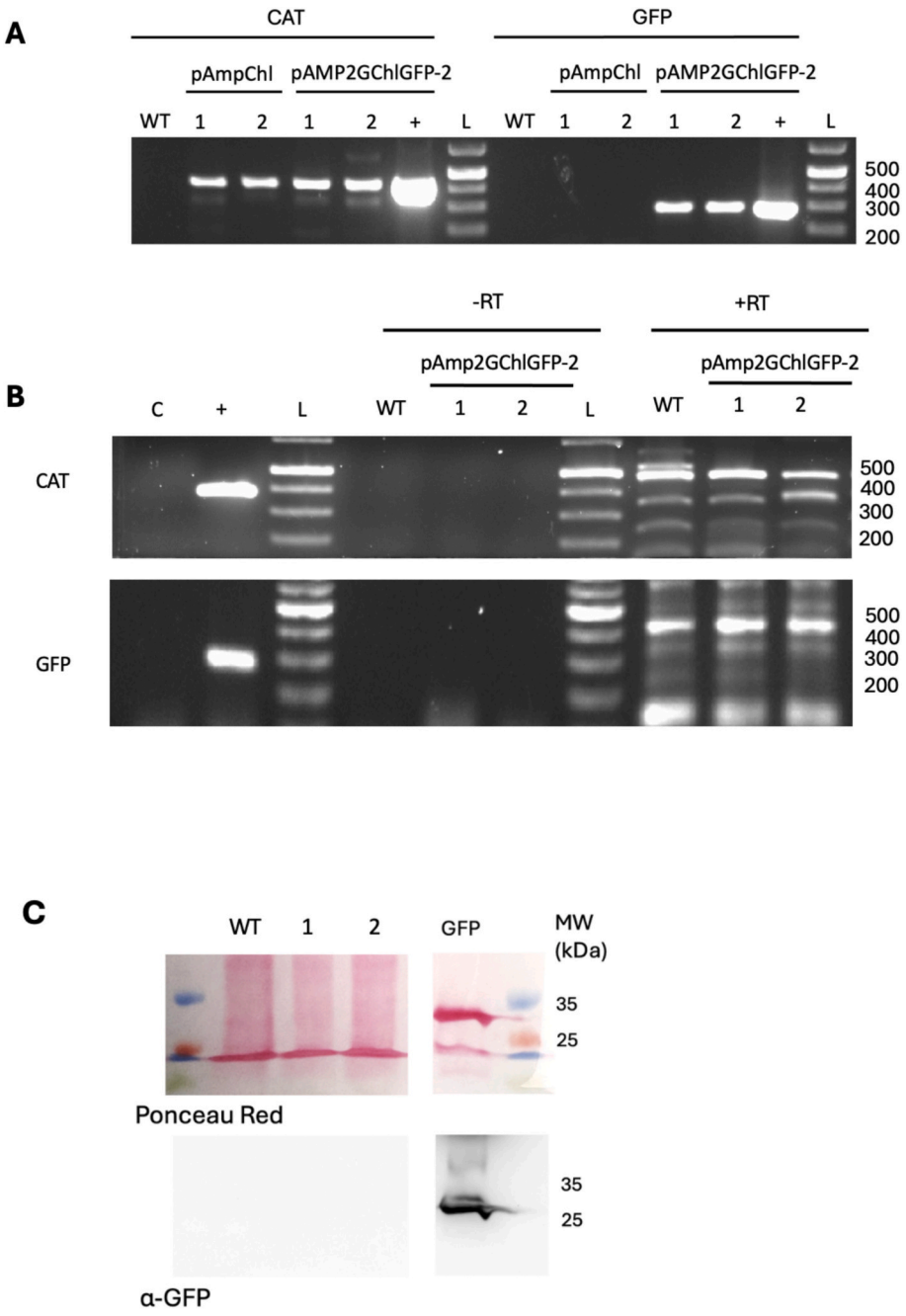

Fig. 7. PCR to confirm successful transformation and RT-PCR and western blot showing that GFP is not expressed. A: PCR. Primers were designed against both CAT and GFP genes (CAT_F1/CAT_R1 and GFP_F1/GFP_R2), and PCR carried out on two separate *A. carterae* cell lines transformed with pAMP2GChlGFP-2. As a control, untransformed *A. carterae* cells (WT), *A. carterae* containing pAmpChl, and purified pAMP2GChlGFP-2 plasmid (+) were included. **B: RT-PCR** RNA was extracted from two separate *A. carterae* cell lines transformed with pAMP2GChlGFP-2. cDNA was synthesized using random hexamers, with (+) and without (−) reverse transcriptase (RT). PCR was carried out using CAT_F2/CAT_R3 and GFP_F1/GFP_R2 primers. As a PCR control, untransformed *A. carterae* cells (WT) and purified pAMP2GChlGFP-2 plasmid (+) were included. **C: Western blot**, showing Ponceau Red stained gel and blot probed with anti-GFP antibody. WT: wild type cells (untransformed), 2G1: *A. carterae* transformed with pAMP2GChlGFP-1, 2G2: *A. carterae* transformed with pAMP2GChlGFP-2. GFP: purified GFP protein as positive control. All lanes are from the same original gel and blot (additional lanes removed). (For interpretation of the references to colour in this figure legend, the reader is referred to the web version of this article.)

(Heyno et al., 2009). To test this, we carried out biolistic transformation of *A. carterae* with pAmp2GChlPTOX as before. Following transformation cells were grown in triplicate under high (60 μE m^{-2} s^{-1}) and low (15 μE m^{-2} s^{-1}) light intensities. There was no significant difference in survival time under the two different light intensities, with all cells dead by 14 days as judged by light microscopy. Thus, in total we carried out a total of 33 experiments (11 independent transformation events, each in triplicate), in which cells were transformed with pAmp2GChlPTOX and incubated for 14 days. 27 of these were under the standard light conditions, whilst 3 were under high light conditions, and 3 under low light conditions. In all cases, cells had died by day 14.

4. Discussion

The results presented here provide a significant development in the establishment of transformation technologies for dinoflagellate algae,

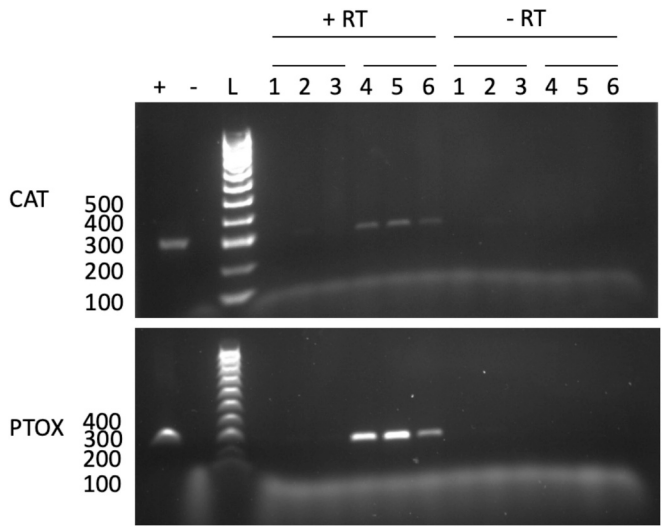

Fig. 8. RT-PCR showing expression of CAT and PTOX genes in *A. carterae.* Expected size of PCR products: CAT 324 bp; PTOX 300 bp. Key: +: positive control for PCR, −: negative control for PCR (no template control), L: Bioline hyperladder 100 bp. Lanes 1–3 are control lines shot with pGEM T-easy (an *E. coli* plasmid) lacking a PTOX gene, Lanes 4–6 are lines shot with pAmpChlPTOX. +/−RT are RT-PCR carried out with/without reverse transcriptase, respectively.

and report on the first attempts at genetic modification to enhance survival of dinoflagellate algae under stress conditions. We have increased the number of *A. carterae* chloroplast transformation vectors to seven, making use of four different native minicircles. We have created artificial minicircles including both a selectable marker and a heterologous gene to allow co-expression of two genes. Although we were not successful in expressing GFP, future research could adapt this vector for expression of other heterologous genes. Finally, we found that the Lonza electroporator is not suitable for use in *A. carterae*.

We attempted to introduce the PTOX gene into *A. carterae,* to see if cells expressing PTOX withstand heat stress conditions more effectively. However, instead we found that the expression of the PTOX gene caused a lethal phenotype. We carried out a total of 33 experiments in which cells were transformed with pAmp2GChlPTOX and incubated for 14 days (27 attempts in the initial experiments, plus 6 under differing light intensities). In all cases, cells had died by day 14. The lack of cellular material meant it was not possible to demonstrate PTOX activity directly. However, the death of cells transformed with pAmp2GChlPTOX alongside the survival of cells transformed with artificial minicircles lacking a PTOX coding sequence, and the demonstration by RT-PCR of PTOX mRNA in cells sacrificed before 14 days, strongly indicate that PTOX was functionally expressed from pAmp2GChlPTOX and caused cell death. Previous studies have suggested that heterologous expression of PTOX surprisingly can lead to increase in reactive oxygen species (Heyno et al., 2009), which would be expected to lead to impaired chloroplast function. Although we do not know why the strains expressing PTOX died, it is consistent with death of the algal cells being due to the effect of PTOX.

Previous studies have shown that the effects of expression of PTOX vary with light intensity and its expression may cause oxidative stress and/or a reduction in photosynthetic yield (Shahbazi et al., 2007; Stepien and Johnson, 2009; Streb et al., 2005). However, our experiments did not indicate any lessening of the deleterious effects at different light intensities. The original two-gene minicircle, based on *petB/atpA,* is known to be represented by abundant transcripts (Dorrell et al., 2019), and so the amount of PTOX produced here may be high, although this has not been verified due to lack of material available for analysis. It is possible that the dinoflagellate response to PTOX production may be beneficial at much lower levels of protein expression, but this is not currently possible with the transformation vectors currently available.

Despite numerous attempts, we were unable to express GFP in *A. carterae.* It is not clear why we were unable to express this protein. Our initial construct pAmp2GChlGFP-1 showed presence of mRNA, while the revised construct pAmp2GChlGFP-2 did not. No GFP was detected by western blot. It should be noted that efforts to obtain stable expression of GFP from the dinoflagellate nuclear genome have also been problematic (Gornik et al., 2022).

Together, these results show the promise of the dinoflagellate chloroplast for the expression of heterologous genes. All four chloroplasts minicircles tested to date have been amenable to genetic modification, suggesting that it would also be possible to use the remaining chloroplast minicircles as shuttle vectors. As dinoflagellate minicircles can include multiple genes, and each minicircle is carried multiple times in the genome, this opens up the possibility for the simultaneous insertion of multiple heterologous genes. Simultaneous expression of multiple heterologous genes in chloroplasts has been challenging in many algal species (Larrea-Alvarez and Purton, 2020). Thus, our advances in developing tools for *A. carterae* chloroplast genome engineering open up new opportunities for research into dinoflagellate chloroplast genetics.

CRediT authorship contribution statement

I.C. Nimmo: Writing – review & editing, Methodology, Investigation. **C.E. Evans:** Writing – review & editing, Methodology, Investigation. **L.M. Li:** Methodology, Investigation. **A.C. Barbrook:** Writing – review & editing, Methodology, Investigation. **K. Geisler:** Resources, Methodology. **F.H. Kleiner:** Writing – review & editing, Methodology, Investigation. **A. Scarampi:** Software, Investigation. **D. Kosmützky:** Software, Methodology, Data curation. **L.T. Wey:** Methodology, Conceptualization. **R.G. Dorrell:** Writing – review & editing, Methodology, Investigation, Formal analysis, Data curation. **C.J. Howe:** Writing – review & editing, Project administration, Methodology, Funding acquisition, Conceptualization. **R.E.R. Nisbet:** Writing – review & editing, Writing – original draft, Project administration, Methodology, Investigation, Funding acquisition, Conceptualization.

Declaration of competing interest

The authors declare the following financial interests/personal relationships which may be considered as potential competing interests: Nisbet, RER and Howe CJ are joint Editors in Chief for Protist. Dorrell RG is Editor for the Dinoflagellate special edition, Protist 2026.

Acknowledgements

This research was funded by the Gordon and Betty Moore Foundation (GBMF4976.01 and GBMF9358) to CJH and RERN. CJH and RERN also acknowledge NERC (UKRI) grant NE/X010503/1 and Leverhulme Trust grant RPG-2025-195. DGK was funded by Gates Cambridge Trust and the Benn W Levy Trust, AS by a BBSRC studentship BB/M011194/1, and LTW by The Cambridge Trust. KG was funded by BBSRC (UKRI) grants BB/L014130/1 and BB/R021694/1. LML is a student from the FIRE PhD program funded by the Bettencourt Schueller foundation and the EURIP graduate program (ANR-17-EURE-0012). RGD acknowledges support from an ERC Starting Grant ('ChloroMosaic', grant number 101039760), awarded 2023-2028.

Appendix A. Supplementary data

Supplementary data to this article can be found online at https://doi.org/10.1016/j.protis.2026.126159.

Data availability

All data shared in suppl. data sections

References

Ahmad, N., Michoux, F., Nixon, P.J., 2012. Investigating the production of foreign membrane proteins in tobacco chloroplasts: Expression of an algal plastid terminal oxidase. PLoS One 7, e41722. https://doi.org/10.1371/JOURNAL.PONE.0041722.

Aquino Cruz, A., Okolodkov, Y.B., 2016. Impact of increasing water temperature on growth, photosynthetic efficiency, nutrient consumption, and potential toxicity of *Amphidinium cf. carterae* and *Coolia monotis* (dinoflagellata) rev. Biol. Mar. Oceanogr. 51, 565–580.

Barbrook, A., Howe, C.J., 2000. Minicircular plastid DNA in the dinoflagellate *Amphidinium operculatum*. Mol. Gen. Genet. 263, 152–158. https://doi.org/10.1007/s004380050042.

Barbrook, A.C., Symington, H., Nisbet, R.E., Larkum, A., Howe, C.J., 2001. Organisation and expression of the plastid genome of the dinoflagellate *Amphidinium operculatum*. Mol. Gen. Genomics. 266, 632–638. https://doi.org/10.1007/s004380100582.

Barbrook, A.C., Santucci, N., Plenderleith, L.J., Hiller, R.G., Howe, C.J., 2006. Comparative analysis of dinoflagellate chloroplast genomes reveals rRNA and tRNA genes. BMC Genomics 7, 297. https://doi.org/10.1186/1471-2164-7-297.

Capella-Gutiérrez, S., Silla-Martínez, J.M., Gabaldón, T., 2009. TrimAl: A tool for automated alignment trimming in large-scale phylogenetic analyses. Bioinformatics 25 (15), 1972–1973.

Chen, J.E., Barbrook, A.C., Cui, G., Howe, C.J., Aranda, M., 2019. The genetic intractability of *Symbiodinium microadriaticum* to standard algal transformation methods. PLoS One 14, e0211936. https://doi.org/10.1371/journal.pone.0211936.

Dinesh Kumar, P.K., Steeven Paul, Y., Muraleedharan, K.R., Murty, V.S.N., Preenu, P.N., 2016. Comparison of long-term variability of sea surface temperature in the arabian sea and bay of bengal. Reg. Stud. Mar. Sci. 3, 67–75 doi.org/10.1016/j.rsma.2015.05.004.

Dorrell, R.G., Klinger, C.M., Newby, R.J., Butterfield, E.R., Richardson, E., Dacks, J.B., Howe, C.J., Nisbet, E.R., Bowler, C., 2017. Progressive and biased divergent evolution underpins the origin and diversification of peridinin dinoflagellate plastids. Mol. Biol. Evol. 34 (2), 361–379. https://doi.org/10.1093/molbev/msw235.

Dorrell, R.G., Nisbet, R.E.R., Barbrook, A.C., Rowden, S.J.L., Howe, C.J., 2019. Integrated genomic and transcriptomic analysis of the peridinin dinoflagellate *Amphidinium carterae* plastid. Protist 170 (4), 358–373. https://doi.org/10.1016/j.protis.2019.06.001.

Durán-Riveroll, L.M., Juárez, O.E., Okolodkov, Y.B., Mejía-Camacho, A.L., Ramírez-Corona, F., Casanova-Gracia, D., Osorio-Ramírez, M.dC., Cervantes-Urieta, V.A., Cembella, A.D., 2023. Morphological and molecular characterization of the benthic dinoflagellate *Amphidinium* from coastal waters of Mexico. Phycology 3 (2), 305–324. https://doi.org/10.3390/phycology3020020.

Faktorová, D., et al., 2019. Genetic tool development in marine protists: emerging model organisms for experimental cell biology. Nat. Methods 17, 481–494. https://doi.org/10.1101/718239doi.

Foyer, C.H., Hanke, G., 2022. ROS production and signalling in chloroplasts: Cornerstones and evolving concepts. Plant J. 111 (3), 642–661. https://doi.org/10.1111/tpj.15856.

Gierz, S.L., Forêt, S., Leggat, W., 2017. Transcriptomic analysis of thermally stressed *Symbiodinium* reveals differential expression of stress and metabolism genes. Front. Plant Sci. 8, 271. https://doi.org/10.3389/fpls.2017.00271.

Gornik, S.G., Maegele, I., Hambleton, E.A., Voss, P.A., Waller, R.F., Guse, A., 2022. Nuclear transformation of a dinoflagellate symbiont of corals. Front. Mar. Sci. 9, 1035413. https://doi.org/10.3389/fmars.2022.1035413.

Helgoe, J., Davy, S.K., Weis, V.M., Rodriguez-Lanetty, M., 2024. Triggers, cascades, and endpoints: Connecting the dots of coral bleaching mechanisms. Biol. Rev. 99 (3), 715–752 doi.org/10.1111/brv.13042.

Heyno, E., Gross, C.M., Laureau, C., Culcasi, M., Pietri, S., Krieger-Liszky, A., 2009. Plastid alternative oxidase (PTOX) promotes oxidative stress when overexpressed in tobacco. J. Biol. Chem. 284, 31174–31180. https://doi.org/10.1074/JBC.M109.021667.

Howe, C.J., Ellen, R., Nisbet, R., Barbrook, A.C., 2008. The remarkable chloroplast genome of dinoflagellates. J. Exp. Bot. 59, 1035–1045. https://doi.org/10.1093/jxb/erm292.

Joët, T., Genty, B., Josse, E.M., Kuntz, M., Cournac, L., Peltier, G., 2002. Involvement of a plastid terminal oxidase in plastoquinone oxidation as evidenced by expression of the *Arabidopsis thaliana* enzyme in tobacco. J. Biol. Chem. 277 (35), 31623–31630. https://doi.org/10.1074/jbc.M203538200.

Jones, R.J., Ward, S., Amri, A.Y., Hoegh-Guldberg, O., 2000. Changes in quantum efficiency of photosystem II of symbiotic dinoflagellates of corals after heat stress, and of bleached corals sampled after the 1998 Great Barrier Reef mass bleaching event. Mar. Freshw. Res. 51, 63–71. https://doi.org/10.1071/MF99100.

Judd, M., Baldino, A., Wira, J., et al., 2024. Collectors, not hoarders: complex gene structures in *Amphidinium carterae* revealed through nanopore sequencing. BMC Genomics 26, 992. https://doi.org/10.1186/s12864-025-12184-7.

Katoh, K., Standley, D.M., 2013. MAFFT multiple sequence alignment software version 7: Improvements in performance and usability. Mol. Biol. Evol. 30 (4), 772–780. https://doi.org/10.1093/molbev/mst010.

LaJeunesse, T.C., Parkinson, J.E., Gabrielson, P.W., Jeong, H.J., Reimer, J.D., Voolstra, C.R., Santos, S.R., 2018. Systematic revision of *Symbiodiniaceae* highlights the antiquity and diversity of coral endosymbionts. Curr. Biol. 28 (16), 2570–2580. e6. https://doi.org/10.1016/j.cub.2018.07.008.

Larrea-Alvarez, M., Purton, S., 2020. Multigenic engineering of the chloroplast genome in the green alga *Chlamydomonas reinhardtii*. Microbiology (Reading) 166 (6), 510–515. https://doi.org/10.1099/mic.0.000910.

Lennon, A.M., Prommeenate, P., Nixon, P.J., 2003. Location, expression and orientation of the putative chlororespiratory enzymes, ndh and IMMUTANS, in higher-plant plastids. Planta 218, 254–260. https://doi.org/10.1007/S00425-003-1111-7.

Lilley, R.M., Ralph, P.J., Larkum, A.W.D., 2010. The determination of activity of the enzyme RuBisCo in cell extracts of the dinoflagellate alga *Symbiodinium* sp. by manganese chemiluminescence and its response to short-term thermal stress of the alga. Plant Cell Environ. 33, 995–1004. https://doi.org/10.1111/J.1365-3040.2010.02121.X.

Lin, S., 2024. A decade of dinoflagellate genomics illuminating an enigmatic eukaryote cell. BMC Genomics 25 (1), 932. https://doi.org/10.1186/s12864-024-10847-5.

Muscatine, L., Porter, J.W., 1977. Reef corals: Mutualistic symbioses adapted to nutrient-poor environments. Bioscience 27, 454–460. https://doi.org/10.2307/1297526.

Nguyen, L.T., Schmidt, H.A., von Haeseler, A., Minh, B.Q., 2015. IQ-TREE: A fast and effective stochastic algorithm for estimating maximum-likelihood phylogenies. Mol. Biol. Evol. 32 (1), 268–274. https://doi.org/10.1093/molbev/msu300.

Nimmo, I.C., Barbrook, A.C., Lassadi, I., Chen, J.E., Geisler, K., Smith, A.G., Aranda, M., Purton, S., Waller, R.F., Nisbet, R.E.R., Howe, C.J., 2019. Genetic transformation of the dinoflagellate chloroplast. Elife 8, e45292. https://doi.org/10.7554/eLife.45292.

Perrin, A.J., Dorrell, R.G., 2024. Protists and protistology in the anthropocene: challenges for a climate and ecological crisis. BMC Biol. 22, 279. https://doi.org/10.1186/s12915-024-02077-8.

Ragni, M., Airs, R.L., Hennige, S.J., Suggett, D.J., Warner, M.E., Geider, R.J., 2010. PSII photoinhibition and photorepair in *Symbiodinium* (pyrrhophyta) differs between thermally tolerant and sensitive phylotypes. Mar. Ecol. Prog. Ser. 406, 57–70. https://doi.org/10.3354/MEPS08571.

Reis, A.C., Salis, H.M., 2020. An automated model test system for systematic development and improvement of gene expression models. ACS Synth. Biol. 9 (11), 3145–3156. https://doi.org/10.1021/acssynbio.0c00394.

Rosso, D., Ivanov, A.G., Fu, A., Geisler-Lee, J., Hendrickson, L., Geisler, M., Stewart, G., Krol, M., Hurry, V., Rodermel, S.R., Maxwell, D.P., Hüner, N.P.A., 2006. IMMUTANS does not act as a stress-induced safety valve in the protection of the photosynthetic apparatus of arabidopsis during steady-state photosynthesis. Plant Physiol. 142, 574–585. https://doi.org/10.1104/PP.106.085886.

Shahbazi, M., Gilbert, M., Labouré, A.M., Kuntz, M., 2007. Dual role of the plastid terminal oxidase in tomato. Plant Physiol. 145, 691. https://doi.org/10.1104/PP.107.106336.

Sprecher, B.N., Zhang, H., Lin, S., 2020. Nuclear gene transformation in the dinoflagellate *Oxyrrhis marina*. Microorganisms 8 (1), 126. https://doi.org/10.3390/microorganisms8010126.

Stepien, P., Johnson, G.N., 2009. Contrasting responses of Photosynthesis to salt stress in the glycophyte *Arabidopsis* and the halophyte *Thellungiella*: Role of the plastid terminal oxidase as an alternative electron sink. Plant Physiol. 149, 1154–1165. https://doi.org/10.1104/PP.108.132407.

Streb, P., Josse, E.M., Gallouët, E., Baptist, F., Kuntz, M., Cornic, G., 2005. Evidence for alternative electron sinks to photosynthetic carbon assimilation in the high mountain plant species ranunculus glacialis. Plant Cell Environ. 28, 1123–1135. https://doi.org/10.1111/J.1365-3040.2005.01350.X.

Szabó, M., Larkum, A.W.D., Vass, I., 2020. A Review: The role of Reactive Oxygen Species in mass coral bleaching. In: Photosynthesis in Algae: Biochemical and Physiological Mechanisms. Springer, pp. 459–488. https://doi.org/10.1007/978-3-030-33397-3_17.

Tang, Y.Z., Dobbs, F.C., 2007. Green autofluorescence in dinoflagellates, diatoms, and other microalgae and its implications for vital staining and morphological studies. Appl. Environ. Microbiol. 73 (7), 2306–2313.

Vaulot, D., Sim, C.W.H., Ong, D., Teo, B., Biwer, C., Jamy, M., Lopes Dos Santos, A., 2022. MetaPR2 : a database of eukaryotic 18S rRNA metabarcodes with an emphasis on protists. Mol. Ecol. Resour. 22 (8), 3188–3201. https://doi.org/10.1111/1755-0998.13674.

Vernette, C., Henry, N., Lecubin, J., de Vargas, C., Hingamp, P., Lescot, M., 2021. The ocean barcode atlas: A web service to explore the biodiversity and biogeography of marine organisms. Mol. Ecol. Resour. 21 (4), 1347–1358.

Wangersky, P., Guillard, R., 1960. Low molecular weight organic base from the dinoflagellate *Amphidinium carteri*. Nature 185, 689–690.

Warner, M.E., Fitt, W.K., Schmidt, G.W., 1999. Damage to photosystem II in symbiotic dinoflagellates: A determinant of coral bleaching. Proc. Natl. Acad. Sci. 96, 8007–8012. https://doi.org/10.1073/pnas.96.14.8007.

Weis, V.M., 2008. Cellular mechanisms of cnidarian bleaching: stress causes the collapse of symbiosis. J. Exp. Biol. 211 (Pt 19), 3059–3066. https://doi.org/10.1242/jeb.009597.